

# Lawrence Berkeley National Laboratory

## LBL Publications

### Title

Anaerobic Dynamic Membrane Bioreactor Development to Facilitate Organic Waste Conversion to Medium-Chain Carboxylic Acids and Their Downstream Recovery

### Permalink

<https://escholarship.org/uc/item/7qv052k9>

### Journal

ACS ES&T Engineering, 2(2)

### ISSN

2690-0645

### Authors

Shrestha, Shilva  
Xue, Siqi  
Kitt, Dianna  
[et al.](#)

### Publication Date

2022-02-11

### DOI

10.1021/acsestengg.1c00273

Peer reviewed

# Anaerobic Dynamic Membrane Bioreactor Development to Facilitate Organic Waste Conversion to Medium-Chain Carboxylic Acids and Their Downstream Recovery

Shilva Shrestha, Siqui Xue, Dianna Kitt, Hang Song, Caro Truyers, Maxim Muermans, Ilse Smets, and Lutgarde Raskin\*

Cite This: <https://doi.org/10.1021/acsestengg.1c00273>

Read Online

ACCESS |

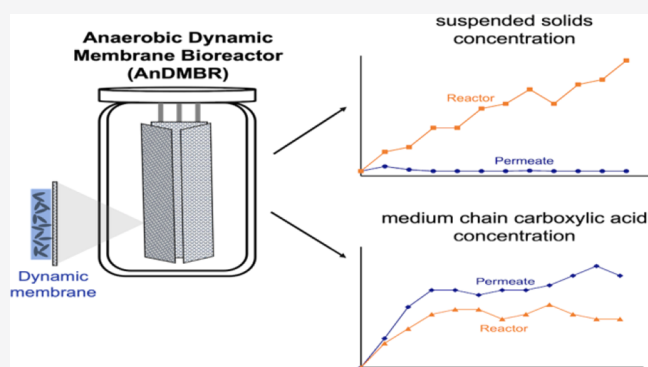
Metrics & More

Article Recommendations

Supporting Information

**ABSTRACT:** Platform chemicals such as medium-chain carboxylic acids (MCCAs) can be produced from organic waste streams via chain elongation in anaerobic mixed-culture bioreactors. A product recovery system is needed to collect MCCAs from the bioreactor effluent. Membrane-based liquid–liquid extraction, the most commonly used product recovery approach, requires suspended solids removal from the bioreactor effluent to avoid membrane fouling. An anaerobic dynamic membrane bioreactor (AnDMBR) was developed to evaluate MCCA production from brewery and prefermented food waste and to produce a permeate with low suspended solids to facilitate downstream product recovery. The AnDMBR employed an inexpensive stainless-steel mesh as the support material for the development of a biofilm or dynamic membrane, which was responsible for solids–liquid separation. The AnDMBR produced a permeate quality with an average total suspended solids (TSS) concentration of  $0.12 \text{ g L}^{-1}$ , while the average bioreactor TSS concentration was two orders of magnitude higher ( $21.6 \text{ g L}^{-1}$ ). A maximum solids removal efficiency of  $\geq 99\%$  was achieved and good permeate quality was sustained for over 200 days without fouling control or cleaning the support material. In addition to solids–liquid separation, the dynamic membrane was responsible for a substantial fraction of the biological activity of the AnDMBR. The relative activity of *Clostridiales*, as determined by 16S rRNA sequencing, correlated with MCCA production and was higher in the dynamic membrane ( $20.0 \pm 4.9\%$ ) than in the suspended biomass ( $5.2 \pm 2.7\%$ ) in the bioreactor. This observation was consistent with MCCA production data as the permeate MCCA concentrations were significantly ( $p = 8.2 \times 10^{-5}$ ) higher than that in the bioreactor, suggesting that the dynamic membrane biofilm contributed to chain elongation.

**KEYWORDS:** chain elongation, brewery waste, membrane bioreactor, biofilm, microbial community



## INTRODUCTION

The recovery of medium-chain carboxylic acids (MCCAs) from organic waste streams via chain elongation has gained attention as an alternative to traditional palm kernel oil or coconut oil routes of MCCA production.<sup>1–5</sup> MCCAs are platform chemicals used in the production of lubricants, fragrances, dyes, and fuels, and as livestock feed additives and antimicrobial agents.<sup>1</sup> Chain elongation is a microbial metabolic pathway involving step-wise lengthening of the carbon chain of short-chain carboxylic acids (SCCAs, C1–C5) using electron rich compounds (e.g., ethanol) into longer chain MCCAs (C6–C12), such as caproic acid (C6), enanthic acid (C7), and caprylic acid (C8), via the reverse  $\beta$  oxidation pathway.<sup>1</sup> While SCCAs, which are readily produced during anaerobic fermentation, are valuable, they are difficult to extract because of their high hydrophilicity, while the hydrophobic nature of MCCAs facilitates downstream

recovery.<sup>6</sup> Furthermore, upon chemical conversion, the longer chain MCCAs yield higher molecular weight, energy-dense products<sup>7</sup> compared to SCCAs making MCCAs more valuable than SCCAs. MCCA production via chain elongation has been demonstrated using a variety of anaerobic mixed microbial communities as inocula, including biomass derived from anaerobic digesters,<sup>7,8</sup> chain elongation bioreactors,<sup>2,9</sup> and marine sediment,<sup>10</sup> as well as pure cultures such as *Clostridium kluveri*,<sup>11</sup> *Eubacterium pyruvativorans*,<sup>12</sup> *Eubacterium limosum*,<sup>13</sup> and *Megasphaera elsdenii*.<sup>14</sup>

**Received:** July 22, 2021

**Revised:** November 6, 2021

**Accepted:** November 12, 2021

A product recovery system needs to be operated downstream of the chain elongation bioreactor to yield MCCAs in a commercially usable form. MCCAs can be recovered from the chain elongation bioreactor with an in-line extraction unit, also referred to as in-situ product recovery, or in batch mode from the bioreactor effluent. In addition to removing the MCCAs from the bioreactor and concentrating them, unconsumed precursors such as SCCAs and other soluble products are removed during this process. Removing MCCAs from the bioreactor also helps to alleviate product toxicity caused by the undissociated forms of MCCAs.<sup>1</sup> Since chain elongation bioreactors are operated at pH values close to the  $pK_a$  of the MCCAs, undissociated MCCAs are commonly present at concentrations sufficiently high to be inhibitory for microorganisms (for example, 3.2–7.5 mM of undissociated caproic acid at pH 5.5).<sup>3,15</sup> Furthermore, since MCCA toxicity increases with the carbon-chain length, continuous MCCA removal provides a selective advantage for the formation of the longest possible MCCAs.<sup>6</sup> Lastly, the continuous removal of MCCAs is beneficial because it reduces the amount of base needed for bioreactor buffering.

Membrane-based liquid–liquid extraction (i.e., pertraction) is the most commonly used product recovery approach in chain elongation systems and has shown promising MCCA extraction efficiencies greater than 90%.<sup>2–4,7,9,16</sup> It is important to remove suspended solids from the bioreactor effluent prior to downstream extraction to avoid membrane fouling, which otherwise increases mass transfer resistance and decreases extraction efficiency.<sup>17</sup> Most chain elongation studies use multiple external filters before the extraction step to remove suspended solids.<sup>2,4,7,9,16</sup> The use of external filtration steps results in biomass loss from the chain elongation bioreactor and increases capital and operating costs. The use of a membrane bioreactor for MCCA production and simultaneous suspended solids removal would make it possible to directly integrate MCCA production with downstream separation processes. Anaerobic membrane bioreactors (AnMBRs) using microfiltration or ultrafiltration membranes have been widely applied in wastewater treatment processes. However, they have several disadvantages, including low flux, high capital and operating costs, rapid membrane fouling, and high energy and chemical consumption for membrane cleaning.<sup>18,19</sup> Anaerobic dynamic membrane bioreactors (AnDMBRs) have the potential to address some of these shortcomings. Operation of an AnDMBR depends on the in-situ formation of a biological cake layer, also referred to as a dynamic membrane, on a support surface to provide effective filtration.<sup>20–22</sup> Materials such as stainless-steel meshes as well as woven and nonwoven fabrics, with pore sizes typically ranging from 5 to 200  $\mu\text{m}$ , serve as the support for the development of dynamic membranes. Dynamic membranes have a lower porosity than the support material, providing improved filtration.<sup>20,21</sup> Low cost, high flux, ease of fouling control, and low energy requirements make AnDMBR a promising technology.<sup>20,21</sup> However, the AnDMBR is still in its infancy and additional advances are needed to improve the permeate quality and to fully understand the physicochemical and microbiological factors affecting dynamic membrane formation and properties.

The versatility of AnDMBR systems has been demonstrated for the production of biogas, lactic acid, and SCCAs from diverse waste streams, including domestic wastewater, food waste, cheese whey wastewater, and landfill leachate,<sup>23–27</sup> but not yet for the production of MCCAs. Previous studies have

demonstrated that AnDMBRs can produce an effluent (permeate) with total suspended solids (TSS) level less than 10  $\text{mg L}^{-1}$ .<sup>28,29</sup> With such efficient solids–liquid separation, AnDMBRs provide the potential to produce an effluent that can be sent directly to a membrane-based extraction system for MCCA recovery, thus avoiding external filtration steps. The integration of AnDMBRs with downstream extraction systems is expected to reduce cost, environmental impacts, and physical footprints of chain elongation bioreactor systems. Furthermore, AnDMBRs offer the potential for improved biomass retention, which is important to achieve high conversion rates for MCCA production and resilience toward upsets.<sup>30–32</sup> Improved biomass retention in chain elongation systems so far has been studied in granular sludge-based processes and through cell immobilization on carrier materials in up-flow anaerobic filters.<sup>9,30–34</sup> The potential of AnDMBRs for MCCA production with simultaneous suspended solids removal and improved biomass retention has not been explored previously.

A bench-scale AnDMBR equipped with flat sheet stainless-steel meshes was developed to promote dynamic membrane formation for solids–liquid separation to facilitate downstream MCCA extraction and biomass retention. The AnDMBR was fed with a mixture of ethanol-rich waste beer and SCCA-rich permeate from a bioreactor treating food waste. The objectives of this study were to develop and evaluate the applicability of AnDMBR technology for MCCA production and effective solids–liquid separation. We evaluated the factors affecting its performance and characterized the contribution of the dynamic membrane biofilm in MCCA production.

## ■ MATERIALS AND METHODS

**Bioreactor Influent and Inoculum.** The bioreactor influent was composed of ethanol-rich waste beer and a SCCA-rich permeate collected from an acidogenic bioreactor treating food waste.<sup>35</sup> Waste beer is a waste stream produced in breweries as a result of failure to meet quality standards, development of off flavors, improper fermentation or storage, and includes beer past its expiration date.<sup>36</sup> The influent ratio of permeate to waste beer was determined by using the stoichiometric equations for chain elongation (4:1 for ethanol:acetate, 2.4:1 for ethanol:propionate, 1.2:1 ethanol:butyrate, and 1.2:1 ethanol:valerate).<sup>1</sup>

The bioreactor was inoculated with rumen content collected from a fistulated cow at the Michigan State University dairy farm (East Lansing, MI, USA). The bioreactor was reinoculated with a mixture of rumen content and biomass from a separate chain elongation bioreactor<sup>15</sup> (referred to as adapted chain elongation inoculum) on Day 175. The characteristics of the waste beer, permeate, and different inocula are provided in Table S1.

**Bioreactor System and Operating Condition.** The AnDMBR consisted of a 7-L bioreactor (Chemglass Life Sciences, Vineland, NJ, USA) with a working volume of 4.8 L. The bioreactor was equipped with three submerged rectangular membrane modules with each module containing two flat sheet stainless-steel meshes (TWP, Berkeley, CA, USA) with an area of 0.0163  $\text{m}^2$ . The AnDMBR system included peristaltic pumps for feeding and permeation, which were remotely controlled using LabVIEW (National Instruments, Austin, TX, USA) data acquisition software. The bioreactor was continuously stirred with an overhead impeller (Scilogex, Rocky Hill, CT, USA) and was continually fed from a well-mixed and refrigerated influent reservoir. A 5-L Tedlar

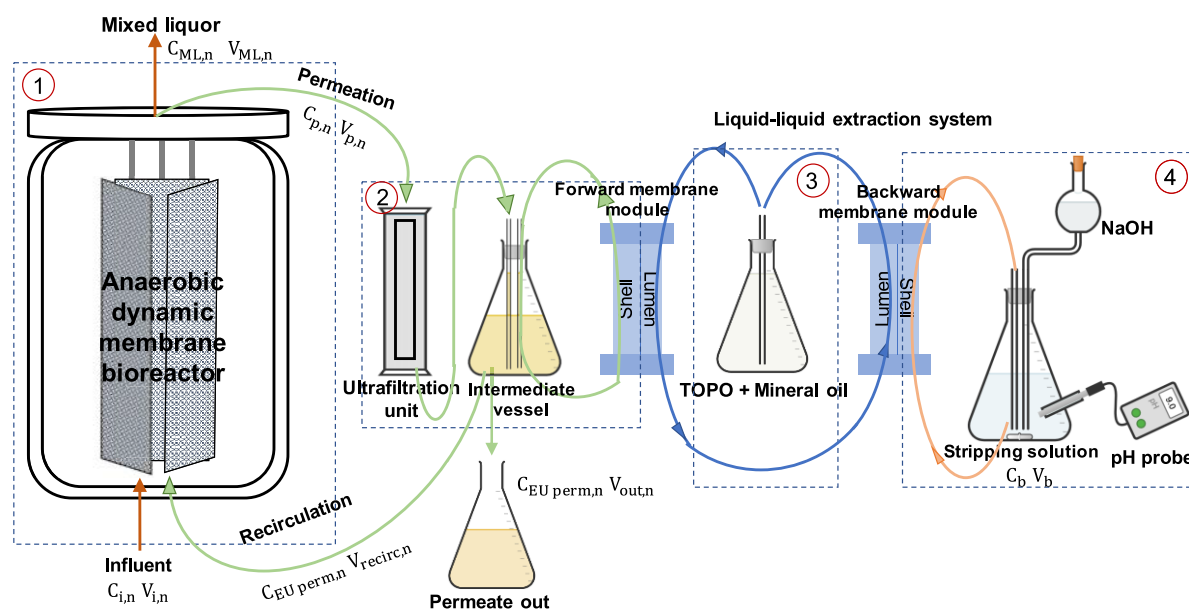


**Figure 1.** Schematic representation of the AnDMBR integrated with the liquid–liquid extraction system labeled with flows in and out of each unit process. 1, 2, 3, and 4 represent system boundaries for the mass balance calculation presented in SI eq S6. Ultrafiltration unit was implemented on Day 245 as an additional barrier during instances of sloughing of the dynamic membrane layer.

**Table 1. Summary of AnDMBR Experimental Phases, Operating Conditions, and Performance<sup>a</sup>**

| Phases                                   | Phase 1           |                  |                            | Phase 2           |                    | Phase 3            | Phase 4           |                            |
|--|-------------------|------------------|----------------------------|-------------------|--------------------|--------------------|-------------------|----------------------------|
|  | Phase 1A          | Phase 1B         | Phase 1C                   | Phase 2A          | Phase 2B           |                    | Phase 4A          | Phase 4B                   |
| filtration mode                          | semicontinuous    | continuous       |                            | continuous        |                    | continuous         | continuous        |                            |
| mesh pore size ( $\mu\text{m}$ )         |                   | 25               |                            | 25                |                    | 25                 | 5                 |                            |
| flux ( $\text{L m}^{-2} \text{h}^{-1}$ ) | N.A.              | $0.5 \pm 0.07$   | $0.6 \pm 0.05$             | $0.7 \pm 0.05$    | $0.6 \pm 0.08$     | $0.7 \pm 0.05$     | $0.6 \pm 0.07$    | $0.4 \pm 0.15$             |
| influent change                          |                   |                  | unintentional TSS increase |                   | centrifuged        |                    |                   | centrifuged+noncentrifuged |
| influent TSS ( $\text{g L}^{-1}$ )       | $1.60 \pm 0.51$   | $3.08 \pm 2.20$  | $9.73 \pm 2.72$            | $10.23 \pm 0.91$  | $1.73 \pm 0.86$    | $1.50 \pm 0.40$    | $1.33 \pm 0.39$   | $3.29 \pm 0.87$            |
| reactor TSS ( $\text{g L}^{-1}$ )        | $6.22 \pm 3.39$   | $18.17 \pm 7.23$ | $35.87 \pm 3.86$           | $29.67 \pm 5.14$  | $26.78 \pm 8.70$   | $12.17 \pm 2.45$   | $11.68 \pm 1.85$  | $19.13 \pm 4.65$           |
| permeate TSS ( $\text{g L}^{-1}$ )       | $0.81 \pm 0.52$   | $0.11 \pm 0.06$  | $0.22 \pm 0.15$            | $0.41 \pm 0.45$   | $0.20 \pm 0.15$    | $0.85 \pm 0.38$    | $0.47 \pm 0.14$   | $0.17 \pm 0.08$            |
| permeate turbidity (NTU)                 | $554.2 \pm 401.3$ | $42.3 \pm 62.9$  | $80.8 \pm 95.5$            | $275.5 \pm 681.1$ | $36.2 \pm 13.9$    | $1693.9 \pm 981.5$ | $953.3 \pm 978.2$ | $73.1 \pm 146.0$           |
| TSS removal (%)                          | $55.8 \pm 23.9$   | $93.9 \pm 5.7$   | $97.8 \pm 1.3$             | $96.1 \pm 4.3$    | $85.0 \pm 13.1$    | $42.5 \pm 31.7$    | $61.8 \pm 12.4$   | $94.2 \pm 2.7$             |
| days                                     | 1–49              | 50–233<br>1–284  | 234–284                    | 285–312           | 313–334<br>285–334 | 335–364            | 365–393           | 394–435<br>365–435         |

<sup>a</sup>N.A., not available; TSS, total suspended solids.

gas bag was connected to the bioreactor headspace for gas collection. The transmembrane pressure (TMP) of each membrane module was continuously recorded starting from Day 282 using pressure sensors (Ashcroft, Stratford, CT, USA) and LabVIEW. A schematic representation of the AnDMBR system is shown in Figure 1.

The bioreactor was operated at  $37^\circ\text{C}$  and a pH of  $5.5 \pm 0.1$  was maintained by the addition of 3 M NaOH controlled with LabVIEW. The hydraulic retention time (HRT) was maintained at  $4.2 \pm 0.8$  days and the organic loading rate varied from 2.7 to 18.0 g soluble chemical oxygen demand (sCOD)  $\text{L}^{-1} \text{d}^{-1}$  over the course of the experiment (Table S2). The solids retention time (SRT) was calculated by dividing the suspended biomass in the bioreactor measured as volatile

suspended solids (VSS) by the amount of biomass lost through the permeate per time unit. Note that this SRT calculation did not consider attached biomass.

The AnDMBR operating time was divided into four phases (Table 1). In Phase 1 (Days 1–284), stainless-steel meshes with a pore size of  $25 \mu\text{m}$  were used as the support material with no fouling control until Day 274. The filtration mode was semicontinuous until Day 49 (Phase 1A, Days 1–49) with frequent backwashing after which it was switched to continuous filtration without backwashing (Phase 1B, Days 50–233). Bioreactor content wasting ( $0.4 \pm 0.3$  L, one to two times per week) began on Day 138 to decrease mixed liquor suspended solids (MLSS) concentration. The TSS concentration in the influent increased starting on Day 234 (Phase



1C, Days 234–284) because of an increase in the TSS concentration of the SCCA-rich permeate. The meshes were replaced with a new set of 25  $\mu\text{m}$  meshes on Day 285, which was the start of Phase 2 (Days 285–334). Starting on Day 313 (Phase 2B, Days 313–334), the SCCA-rich permeate was centrifuged (10,000  $\times g$  for 10 min) and the supernatant was used to prepare the AnDMBR influent. To evaluate the effect of lower influent TSS with unfouled meshes, a new set of 25  $\mu\text{m}$  meshes was used in Phase 3 (Days 335–364). In Phase 4 (Days 365–435), 5  $\mu\text{m}$  meshes were incorporated in the membrane modules to compare performance between different mesh pore sizes. In the later part of Phase 4 (Phase 4B, Days 394–435), the noncentrifuged SCCA-rich permeate was mixed with the supernatant of the centrifuged SCCA-rich permeate at a ratio (v:v) of 30:70 (Days 394–421) and 15:85 (Days 422–435) to increase the TSS concentration in the influent.

**Pertraction System.** The pertraction system was similar to the one developed by Kucek et al.<sup>2</sup> It consisted of two hollow-fiber, hydrophobic membrane contactors (Liqui-Cel EXF 2.5\*8, X40) from 3 M (Charlotte, NC, USA). Starting on Day 245, the bioreactor permeate was passed through an ultrafiltration membrane (GE healthcare, PA, USA, 0.03  $\mu\text{m}$  pore size, 0.53  $\text{m}^2$  membrane area), collected in an intermediate vessel, and recirculated through the shell side of the forward membrane contactor at a flow rate of 140  $\text{L d}^{-1}$  (Figure 1). A hydrophobic solvent consisting of mineral oil (Sigma Aldrich, St. Louis, MO, USA) and 30  $\text{g L}^{-1}$  trioctylphosphine oxide (TOPO) was recirculated continuously through the lumen of the forward and backward membrane modules to selectively extract MCCAs. An alkaline stripping solution made up of sodium tetraborate and boric acid was used to back extract MCCAs from the hydrophobic solvent. The in-line extraction system was integrated with the bioreactor and operated from Days 245–270, Days 314–334, and Days 380–435 with some interruptions because of technical difficulties. During Days 380–435, the bioreactor permeate was recirculated continuously at a flow rate of  $3.6 \pm 1.0 \text{ mL min}^{-1}$  between the bioreactor and intermediate vessel while the permeate left the system at a flow rate of  $0.8 \pm 0.1 \text{ mL min}^{-1}$  (Figure 1). Prior to integration with the AnDMBR system, pertraction system trials were run to evaluate the extraction performance with and without TOPO in mineral oil (S2.1, Figure S1, Table S3) and with a synthetic mixture of ethanol, SCCAs, and MCCAs to simulate operation with the real AnDMBR permeate (S2.2, Figure S2). Detailed information on the pertraction system and the trials is provided in the SI Section S1.

**Chemical Analyses.** TSS, VSS, sCOD, and carboxylic acid, lactate, and ethanol concentrations were determined to evaluate the AnDMBR performance. The bioreactor permeate was sampled every 3 days and the bioreactor content and influent were sampled weekly. Inocula samples were collected at each inoculation event. The intermediate vessel permeate and alkaline stripping solution were sampled on the same day of permeate sampling. TSS and VSS were determined according to Standard Methods.<sup>37</sup> sCOD analyses were performed using Lovibond medium-range (0–1500  $\text{mg L}^{-1}$ ) COD digestion vials (Tintometer, Germany). Turbidity was measured with a turbidimeter (Hach 2100 N, Loveland, CO, USA). Gas volume was measured daily with a gas-tight glass syringe. Gas composition was determined using a Gow-Mac Series gas chromatograph (Bethlehem, PA, USA) equipped with a thermal conductivity detector. Carboxylic acid (C2 to

C8, including isoforms of C4 and C5) and ethanol concentrations were determined using an Agilent Technologies 7890B gas chromatograph (Santa Clara, CA) equipped with a Stabilwax-DA column (Restex) and a flame ionization detector. The lactate concentration was measured using an ion chromatograph (ICS-1600, Dionex, Sunnyvale, CA, USA) equipped with a Dionex DX 100 conductivity detector. The gas chromatography conditions are given in the SI. Carboxylic acid values are reported as total carboxylate (sum of dissociated carboxylate and undissociated carboxylic acid).

**Microbial Analyses.** Inocula samples were collected immediately before each inoculation event and influent, bioreactor, and biofilm samples were obtained at various points throughout the experimental period (Table S4) for microbial analyses. Biofilm samples were taken by removing the membrane modules from the bioreactor and scraping the biofilm from the mesh surfaces using a sterile spatula. The samples were centrifuged (10,000  $\times g$  for 10 min at 4  $^{\circ}\text{C}$ ) and the biomass pellet was flash frozen and stored at  $-80 \text{ }^{\circ}\text{C}$ . The cetyltrimethylammonium bromide method was used for DNA extraction as described by Porebski et al.<sup>38</sup> with an additional 1.5 min bead-beating step (Mini-Beadbeater-96, BioSpec Products, Bartlesville, OK, USA). RNA extraction was carried out using TRIzol reagent (Invitrogen, CA, USA) following the manufacturer's instructions with some modifications to include an RNA precipitation step using sodium acetate and ethanol. Extracted DNA and RNA concentrations were determined using a Qubit 2.0 Fluorometer (Invitrogen, Life Technologies, CA, USA). RNA extracts were treated with ezDNase (Thermo Scientific, MA, USA) followed by cDNA synthesis using SuperScript IV VILO cDNA synthesis kit (Invitrogen, Carlsbad, CA).

cDNA and DNA samples were submitted for 16S rRNA and 16S rRNA gene sequencing, respectively, to the Microbial Systems Molecular Biology Laboratory (University of Michigan, Ann Arbor, MI, USA). The V4 region of the 16S rRNA gene was amplified using the primers F515 and R806,<sup>39</sup> which were modified for dual-index sequencing as described by Kozich et al.<sup>40</sup> Sequencing was performed on the Illumina MiSeq platform (San Diego, CA, USA) using the MiSeq Reagent Kit V2 500 cycles. The sequences were processed with DADA2 v1.16<sup>41</sup> in R (version 3.6.1) according to the online pipeline tutorial (SI Section S4). The raw sequences were deposited at the NCBI Sequence Read Archive under BioProject ID PRJNA705381.

**Statistical Analyses.** Statistical analyses of bioreactor performance and microbial community data were performed in R (v.3.6.1) using the vegan (v.2.5.6),<sup>42</sup> phyloseq (v.1.30.0),<sup>43</sup> dplyr (v.1.0.5),<sup>44</sup> DESeq2 (v.1.26.0),<sup>45</sup> and ggplot2 (v.3.3.0)<sup>46</sup> packages. Statistically significant differences between conditions for bioreactor performance data were identified with the Kruskal–Wallis test with Benjamini–Hochberg correction. Pearson correlation coefficients were calculated to determine the correlation between the relative abundance/activity of different microbial ASVs and MCCA production. Nonmetric multidimensional scaling (NMDS) plots were generated using Bray–Curtis distances as implemented in the vegan package to compare the microbial community composition among inocula, influent, bioreactor, and biofilm samples using both DNA and RNA datasets. Analysis of similarities (ANOSIM) was used to determine whether the observed clusters in the NMDS were significantly different. DESeq2<sup>45</sup> using the Wald significance test was used

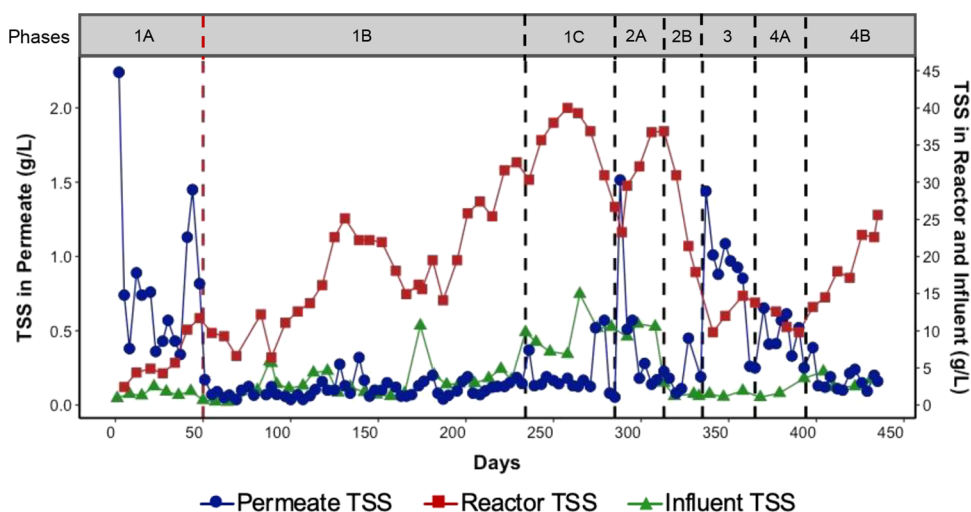


**Figure 2.** Comparison of TSS levels in the permeate, bioreactor (secondary *y*-axis), and influent (secondary *y*-axis) over time. Vertical red dashed line indicates the switch to the continuous filtration mode on Day 50 and the vertical black dashed lines demarcate different experimental phases (Table 1).

to test differential abundance of ASVs read counts between the suspended biomass and corresponding biofilm samples and DNA and RNA microbial data.

## RESULTS AND DISCUSSION

**Dynamic Membrane Produced a High-Quality Permeate despite High TSS in the Bioreactor.** Initially, when the AnDMBR was operated in semi-continuous filtration mode (Phase 1A), the permeate TSS concentration was high ( $0.81 \pm 0.52 \text{ g L}^{-1}$ , Figure 2) suggesting insufficient development of the dynamic membrane. Visual inspection on Day 41 confirmed nonuniform distribution of the cake layer on the support meshes (Figure S3). After switching to continuous filtration mode (Phase 1B), the permeate TSS decreased drastically from  $0.82 \text{ g L}^{-1}$  on Day 48 to  $0.17 \text{ g L}^{-1}$  on Day 51 (Figure 2) with a similar decrease observed in permeate VSS (Figure S4). The TSS removal also improved from 56.3% on Day 48 to 74.3% on Day 51 (Figure S5). Visual inspection on Day 89 showed a uniform distribution of the cake layer on the support meshes (Figure S3). These observations indicate that the formation of a uniform dynamic membrane resulted in effective filtration. The permeate TSS concentration remained below  $0.12 \text{ g L}^{-1}$  and averaged  $0.08 \pm 0.04 \text{ g L}^{-1}$  from Day 50 to 114 with the lowest TSS concentration of  $0.04 \text{ g L}^{-1}$  achieved on Day 69. Similarly, the permeate turbidity remained low with values as low as 7.61 NTU during Phase 1B (Figure S6).

The average MLSS concentration in the bioreactor was  $10.19 \pm 2.71 \text{ g L}^{-1}$  from Day 50 to 114, which was almost two orders of magnitude higher (Figure 2) than the permeate TSS. Given the influent TSS concentration averaged  $2.71 \pm 2.01 \text{ g TSS L}^{-1}$ , a high TSS removal efficiency averaging  $91.5 \pm 8.5\%$  was achieved despite the high TSS concentration in the bioreactor. The ratio of SRT to HRT was  $21.0 \pm 5.2$ , indicating that the AnDMBR successfully decoupled SRT and HRT and effectively retained biomass.

Since AnDMBRs have not been previously studied for MCCA production from high TSS waste streams, we compared the performance of our AnDMBR to AnDMBRs operated in different contexts. For example, some studies have shown that AnDMBRs can produce permeate with a TSS

concentration below  $10 \text{ mg L}^{-1}$  (or turbidity  $<20 \text{ NTU}$ ) when treating low solids feedstocks and for MLSS concentrations of  $5\text{--}8.1 \text{ g L}^{-1}$ .<sup>28,29,47</sup> However, when high TSS waste streams such as food waste were treated in AnDMBRs with high MLSS concentrations of  $20\text{--}45 \text{ g L}^{-1}$ , the permeate TSS levels were much higher ( $\sim 0.8$  to  $2.8 \text{ g TSS L}^{-1}$ ).<sup>23,24</sup> Taken together, these results suggest that careful control of operating conditions is required to produce permeate with low TSS for an extended period (e.g., Phase 1B), which is necessary for the optimal operation of the downstream extraction unit.

**MLSS Concentration and Influent TSS Concentration Affected Dynamic Membrane Formation.** The AnDMBR was operated continuously without removing the dynamic membrane or cleaning the support meshes until Day 274 thus avoiding any chemical or energy use for fouling mitigation. Over this time period, the dynamic membrane likely increased in thickness and compactness. While a mature and stable dynamic membrane is essential to consistently achieve high-quality permeate, it is also important to control the dynamic membrane thickness to limit filtration resistance. Guan et al.<sup>48</sup> showed that a compact dynamic membrane can push the biomass into the pores of the support mesh because of compression, leading to breakdown and dissociation of particles into the permeate. Consistent with this, the permeate TSS concentration in our study started increasing slowly and stayed above  $0.12 \text{ g L}^{-1}$  after Day 114. At the same time, the bioreactor MLSS kept increasing with the MLSS concentration reaching a maximum of  $40.00 \pm 0.35 \text{ g TSS L}^{-1}$  on Day 258 (Figure 2). An unintentional rise in influent TSS concentration (Phase 1C) further increased the MLSS concentration despite frequent biomass wasting (Figure 2, Table 1).

The meshes were replaced with a new set of  $25 \mu\text{m}$  pore size meshes in Phase 2, but the TMP values continued to increase to  $40\text{--}50 \text{ kPa}$  (Figure S7) indicating membrane clogging and the permeate TSS concentration remained high ( $0.35 \pm 0.38 \text{ g L}^{-1}$ ). Changing the meshes again in Phase 3 to evaluate the effect of feeding a low TSS influent still resulted in poor permeate quality ( $0.85 \pm 0.38 \text{ g TSS L}^{-1}$  and  $1693.90 \pm 981.49 \text{ NTU}$ ) (Table 1, Figures 2 and S6). Centrifugation of the influent during Phase 2B likely had a negative effect on bioreactor performance, as centrifugation presumably removed

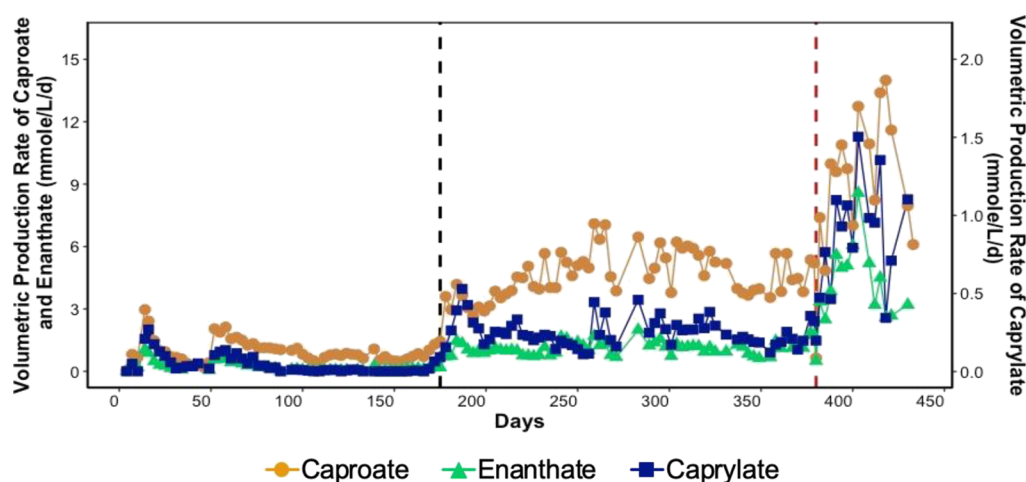


**Figure 3.** Volumetric production rate of caproate, enanthate, and caprylate (secondary *y*-axis) in the bioreactor over time. Vertical black and red dashed lines represent reinoculation with a mixture of rumen and adapted chain elongation inocula on Day 175 and anaerobic dynamic bioreactor (AnDMBR) integration with the extraction unit with recirculation mode on Day 380, respectively. Figure S8 is identical to Figure 3, but includes the different experimental phases (Table 1).

large suspended particles and left mostly particles smaller than the pore size of the support mesh, which had a negative impact on dynamic membrane formation. Additional studies would be necessary to confirm this hypothesis and further determine the impact of influent particle size distribution on dynamic membrane formation.

The decrease in the mesh pore size from 25 to 5  $\mu\text{m}$  at the start of Phase 4 in our study resulted in improved permeate quality ( $0.47 \pm 0.14 \text{ g L}^{-1}$ ) compared to Phase 3. However, the permeate TSS concentration remained higher than in Phases 1 and 2, indicating insufficient development of the dynamic membrane. The mesh pore size impacts permeate quality before the formation of the dynamic membrane and after support mesh cleaning, otherwise permeate quality is primarily determined by the dynamic membrane. A thick and stable dynamic membrane was not formed until Phase 4B. The transition to higher TSS influent in Phase 4B resulted in an increase in the TSS removal efficiency, and a decrease in the permeate TSS concentration and turbidity (Table 1). It should be noted that the influent TSS concentration during Phase 4B was still lower than that during Phases 1C and 2A when the permeate quality began to deteriorate (Table 1).

Overall, we were able to achieve stable performance until Phase 1B, in terms of low permeate TSS after which the change in influent solids characteristics decreased the permeate quality. Both high ( $>9 \text{ g L}^{-1}$ ) and low ( $<1.3 \text{ g L}^{-1}$ ) influent TSS concentrations proved detrimental to the AnDMBR performance. Similarly, a high MLSS concentration can lead to membrane clogging while a low MLSS concentration likely results in slow dynamic membrane formation. Therefore, there is a need to control MLSS within a certain range to optimize AnDMBR performance. Other characteristics of the bioreactor content such as sludge morphology and hydrophobicity have been shown to affect fouling in conventional membrane bioreactors<sup>49</sup> and further study is needed to evaluate these characteristics in dynamic membrane bioreactors. Lastly, previous studies have shown that the pore size of the support material can affect the rate of dynamic membrane formation, permeate quality, and flux.<sup>20,25,50,51</sup> However, the role of mesh pore size was less evident in the current study and needs further investigation.

### Reinoculation and Extraction Unit Integration with AnDMBR Improved MCCA Production.

The MCCA volumetric production rate increased quickly during the first 2 weeks of operation and reached  $4.2 \text{ mmole L}^{-1} \text{ d}^{-1}$  on Day 14. However, MCCA production started decreasing thereafter and stayed low until Day 175 (Figures 3 and S8). On average, the MCCA volumetric production rate was  $1.15 \pm 0.73 \text{ mmole L}^{-1} \text{ d}^{-1}$  from Days 15–175. During this time, only 7% of total sCOD fed was converted to MCCAs. The bioreactor was reinoculated on Day 175 after which MCCA production recovered. A maximum volumetric production rate of  $9.24 \text{ mmole L}^{-1} \text{ d}^{-1}$  was achieved on Day 259 with an average MCCA volumetric production rate of  $5.9 \pm 1.4 \text{ mmole L}^{-1} \text{ d}^{-1}$  from Days 175–379. A maximum yield of  $0.28 \text{ g COD}_{\text{MCCAs}} \text{ g COD}_{\text{in}}^{-1}$  was achieved on Day 184. The remaining influent sCOD was converted into acetate via excessive ethanol oxidation to acetate.<sup>15</sup> A smaller portion of the remaining sCOD fed was also used for gas production, biomass production, and the production of other unmeasured compounds.

The extraction unit was integrated with the AnDMBR and operated in recirculation mode (Figure 1) starting on Day 280. The extraction efficiency averaged  $52.0 \pm 23.2\%$  for the remainder of the operating period (Days 380–435). The MCCA volumetric production rate increased from average values of  $5.9 \pm 1.4 \text{ mmole L}^{-1} \text{ d}^{-1}$  (Days 175–379) to  $13.6 \pm 5.5 \text{ mmole L}^{-1} \text{ d}^{-1}$  (Days 380–435, Figure 3) with a maximum volumetric production rate of  $22.8 \text{ mmole L}^{-1} \text{ d}^{-1}$ . Caproate was the dominant MCCA produced (based on mmole of carbon produced), constituting  $76.6 \pm 8.5\%$  of the total MCCAs, while enanthate and caprylate accounted for  $18.9 \pm 6.5$  and  $4.5 \pm 2.7\%$ , respectively. The continuous recirculation of AnDMBR permeate between the AnDMBR and the intermediate vessel (Figure 1) allowed more time for the unconsumed MCCA precursors like ethanol and acetate still present in the permeate to react in the bioreactor. Furthermore, the continuous removal of MCCAs from the bioreactor likely also decreased MCCA toxicity and contributed to the increased MCCA volumetric production rate as reported in previous studies.<sup>2,3,9</sup> Other chain elongation studies that used complex ethanol waste streams such as



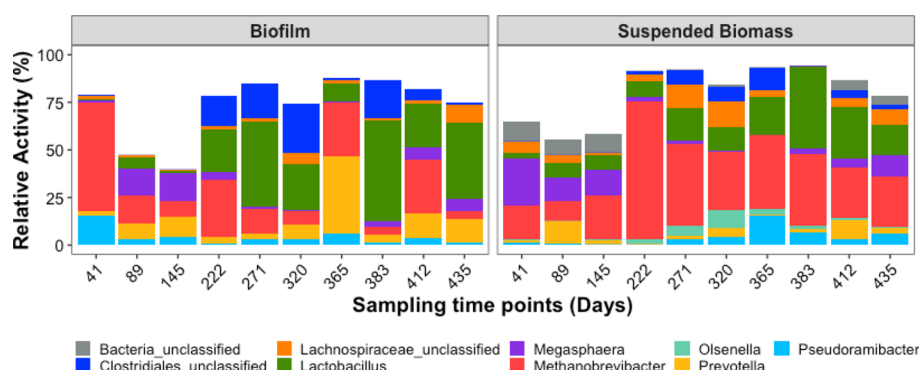


**Figure 4.** Relative activity of the dominant microbial groups active at relative activity greater than 1% in at least 50% of the samples classified to the genus or family level in the biofilm and suspended biomass samples.

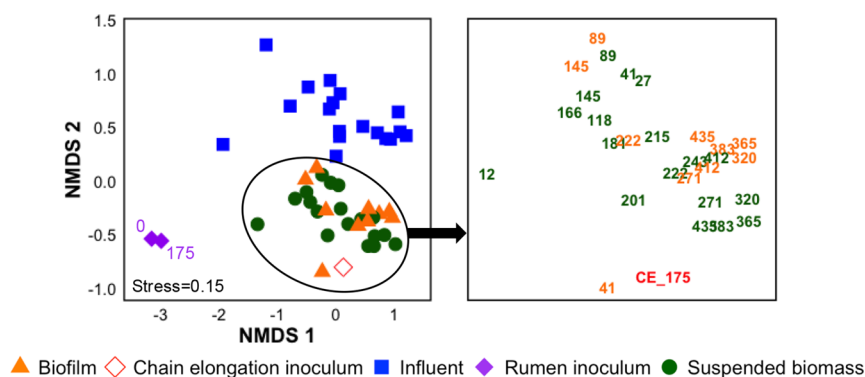


**Figure 5.** NMDS ordination analysis at amplicon sequence variant (ASV) level based on the Bray–Curtis dissimilarity index using 16S rRNA sequencing data in the rumen and chain elongation (CE\_175) inocula and influent, suspended biomass, and biofilm samples. Numbers correspond to sampling time points.

wine lees ( $3.9 \text{ g COD L}^{-1} \text{ d}^{-1}$ )<sup>2</sup> or yeast-fermentation beer ( $7.5 \text{ g COD L}^{-1} \text{ d}^{-1}$ )<sup>3</sup> and employed an in-line extraction unit for continuous MCCA removal have achieved similar or higher MCCA volumetric production rates compared to our study ( $4.0 \pm 1.2 \text{ g COD L}^{-1} \text{ d}^{-1}$ ). Furthermore, Roghair et al.<sup>52</sup> obtained a much higher average caproate volumetric production rate of  $47.3 \text{ mmole L}^{-1} \text{ d}^{-1}$  with fermented food waste and crude ethanol without an in-line extraction process by maintaining a neutral pH compared to our study ( $9.1 \pm 3.4 \text{ mmole L}^{-1} \text{ d}^{-1}$ ).

The AnDMBR produced a low TSS permeate during Phase 1B (Figure 2). This permeate could have been sent to the downstream extraction unit directly. However, when we were ready to connect the extraction unit to the AnDMBR, the permeate quality had deteriorated (Phase 1C). Several changes were made as discussed above to attempt to re-establish stable performance, but the permeate quality remained poor. Therefore, an ultrafiltration unit was installed between the AnDMBR and the extraction unit on Day 245 (Figure 1) to allow us to evaluate the impact of downstream extraction on MCCA production in the AnDMBR while providing protection to the in-line membrane contactors.

**Clostridiales and Pseudoramibacter Populations were Potential MCCA Producers.** The microbial community in the suspended biomass was diverse at the start of bioreactor operation and became dominated by a few microbial groups as bioreactor operation progressed (Figures S9 and S10). The presence of a diverse microbial community during AnDMBR startup possibly resulted in a short startup phase and high MCCA volumetric production rate, which reached  $4.2 \text{ mmole}$

$\text{L}^{-1} \text{ d}^{-1}$  on Day 14. The dominant ASVs in the suspended biomass, determined by 16S rRNA gene sequencing, belonged to unclassified *Bacteria*, *Bulleidia*, unclassified *Clostridiales*, unclassified *Lachnospiraceae*, *Lactobacillus*, *Megasphaera*, *Methanobrevibacter*, *Prevotella*, and *Succiniclasticum* (Figure S11). Based on the 16S rRNA sequencing data, the dominant ASVs belonged to unclassified *Bacteria*, unclassified *Clostridiales*, unclassified *Lachnospiraceae*, *Lactobacillus*, *Megasphaera*, *Methanobrevibacter*, *Olsenella*, *Prevotella*, and *Pseudoramibacter* (Figure 4).

The relative activities of *Clostridiales\_unclassified* (correlation coefficient = 0.54,  $p = 0.02$ ) and *Pseudoramibacter* (correlation coefficient = 0.45,  $p = 0.04$ ) were significantly correlated with the volumetric production rate of MCCAs. The relative abundance and activity of *Clostridiales\_unclassified* on Day 12 were 13.7 and 15.1%, respectively, which corresponded with the high MCCA production observed during the first 2 weeks of operation. Their relative abundance and activity decreased to  $0.5 \pm 0.5$  and  $0.3 \pm 0.3\%$ , respectively, on Day 27 which aligned with the decrease in MCCA production. The partial 16S rRNA gene sequence of ASV 132 was identical to *Clostridium kluyveri*, a model chain elongating bacterium. ASV 132 exhibited a relative activity of 5.9% on Day 12, but it was either not detected at other sampling time points or detected at much lower relative abundance and activity (<1%). Similarly, the relative activity of *Pseudoramibacter* was high at the beginning of bioreactor operation (8.4% on Day 27) when the MCCA production was high after which its relative activity decreased to 1.3% on Day 41.



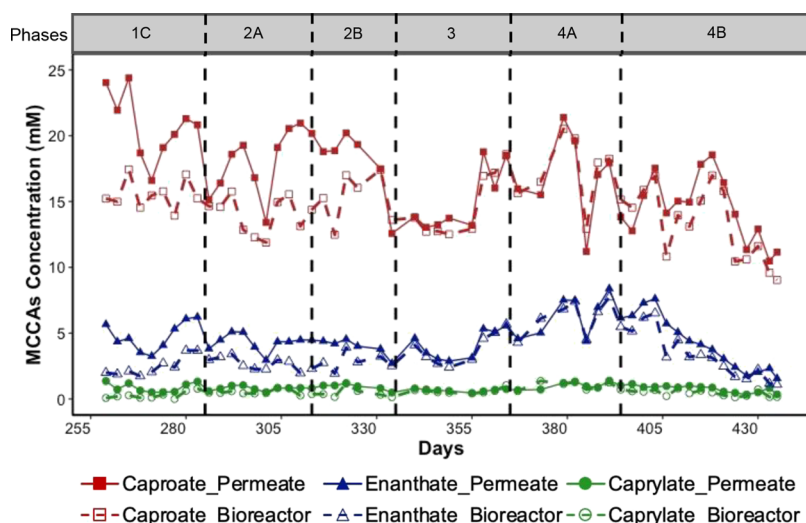


**Figure 6.** Comparison of caproate, enanthate, and caprylate concentrations in permeate and bioreactor samples over time. MCCA concentrations in the bioreactor were measured starting from Day 259. Vertical dashed lines represent different experimental phases (Table 1).

The bioreactor was reinoculated on Day 175 to recover the chain elongation activity and the MCCA production indeed improved immediately after reinoculation. A shift in microbial community structure was observed after reinoculation (Figures 5, S9, S10, and S12). Starting from Day 181, the active microbial community was dominated by *Methanobrevibacter*, *Pseudoramibacter*, *Lactobacillus*, and *Clostridiales\_unclassified*. The relative abundance and activity of both *Clostridiales\_unclassified* and *Pseudoramibacter* increased after reinoculation.

*Clostridiales* and *Pseudoramibacter* were either not detected or detected at low relative abundance and activity in a few influent samples collected over the course of bioreactor operation. *Clostridiales\_unclassified* ASV 7, the dominant ASV in the suspended biomass samples, was present and active in the adapted chain elongation inoculum but had a very low relative activity of 0.005% in the rumen inoculum. The NCBI BLAST<sup>53</sup> analysis of the partial 16S rRNA gene sequence suggests that ASV 7 was most closely related to a previously described chain elongating bacterium, *Eubacterium pyruvativorans*;<sup>12</sup> however, the sequence identity was only 91%. Similarly, *Pseudoramibacter* was not detected in the rumen inocula but was observed at a relative abundance and activity of 0.7 and 0.7%, respectively, in the adapted chain elongation inoculum. *Pseudoramibacter* has been reported in MCCA production from lactate in other mixed-culture studies.<sup>8,54</sup> While the reducing equivalents in the AnDMBR influent primarily consisted of ethanol ( $190.9 \pm 69.9$  mM), a low amount of lactate ( $20.2 \pm 0.6$  mM) derived from the waste beer was also present, which might have promoted lactate chain elongation in addition to ethanol chain elongation. Similarly, *Clostridiales* and *Pseudoramibacter* were found to be dominant during MCCA production using waste beer and prefermented food waste confirming their potential role in chain elongation.<sup>15</sup> Other ethanol-based chain elongation studies have also reported the dominance of members of the *Clostridium* genus when using substrates such as yeast-fermentation beer from the corn ethanol industry<sup>55</sup> and food waste with H<sub>2</sub> and ethanol.<sup>56</sup>

A distinct microbial community developed over time in the bioreactor, independent of the rumen inocula, as shown by the beta-diversity analyses (Figures 5 and S12). The suspended biomass microbial community was more similar to the adapted

chain elongation inoculum than to either of the rumen inocula microbial communities. Several chain elongation studies have used acclimated biomass to inoculate their chain elongation bioreactors.<sup>2,4,16,31,33,34,55</sup> Using an inoculum from a well-functioning and similar system ensures faster startup and shorter acclimation period leading to stable bioreactor performance.<sup>57</sup> Similarly, seeding with an adapted chain elongation inoculum contributed to establishing a stable and active chain elongation community in our study.

**Dynamic Membrane Biofilm Activity Contributed to MCCA Production.** MCCA concentrations were determined in both bioreactor and permeate samples starting from Day 259. The permeate MCCA concentrations, particularly caproate and enanthate, were consistently higher than those in the bioreactor ( $p = 1.14 \times 10^{-9}$ ) from Days 259 to 333 (Figure 6), which suggests that the dynamic membrane was contributing to MCCA production. The difference in MCCA concentrations in the permeate and bioreactor samples aligned with the stability of dynamic membrane formation. For example, the MCCA concentrations in the bioreactor and permeate were similar from Days 334 to 399 ( $p = 0.91$ ), which corresponds to a period of poor solids–liquid separation when the dynamic membrane was not properly formed (qualitatively confirmed by visual observations, permeate TSS concentration, and TSS removal %). The MCCA concentrations were again higher in the permeate than in the corresponding bioreactor samples starting from Day 400 (Figure 6), when a well-formed dynamic membrane was observed (Figure S3), although these differences were not statistically significant ( $p = 0.11$ ).

We compared the microbial community structure in the biofilm and suspended biomass samples (Figures 4 and S11). A few populations, *Methanobrevibacter* (56.9%) and *Pseudoramibacter* (15.8%), dominated in the active biofilm microbial community on Day 41. The Day 41 biofilm sample was most dissimilar compared to other samples (Figure 5). The active biofilm microbial community had changed by Day 89 (Figures 4 and 5) when continuous filtration had led to a well-formed dynamic membrane (Phase 1B) possibly affecting the biofilm microbial community. The active biofilm microbial community had again changed by Day 222 as a result of the reinoculation event on Day 175 (Figures 4 and 5). The suspended biomass communities showed similar shifts although there were

differences in relative abundances of some microbial populations between biofilm and suspended biomass communities (Figures 4 and S11).

*Lactobacillus* was active in the biofilm throughout the operating period with varying relative abundance (0.6–11.2%) and activity (0.4–45.0%). Its relative activity was particularly high starting from Day 383 (22.7–53.4%), possibly as a result of changing the mesh pore size from 25 to 5  $\mu\text{m}$  on Day 365. *Lactobacillus* produces extracellular polymeric substances (EPSs) as a metabolic product of carbohydrate degradation.<sup>58</sup> As EPSs play an important role in microbial biofilm formation by promoting cell aggregation and adhesion in the dynamic membrane,<sup>47,59,60</sup> the enrichment of *Lactobacillus* may have contributed to the development of the dynamic membrane.

The data in Figure 4 as well as the beta-diversity results in Figure 5 showed that the active biofilm and suspended biomass communities were quite different on Day 41 but became more similar to each other with time (ANOSIM  $R = 0.11$ ,  $p = 0.06$ ). Nonetheless, the relative activity of *Clostridiales* unclassified, which was positively correlated to MCCA production, still differed greatly between the suspended biomass and biofilm samples, particularly during the period when permeate MCCA concentrations were significantly higher than the corresponding bioreactor concentrations. From Days 222–320, *Clostridiales* unclassified was found at a higher relative activity in the biofilm samples ( $20.0 \pm 4.9\%$ ) than in the suspended biomass samples ( $5.2 \pm 2.7\%$ ), thus corroborating the MCCA data. These observations indicate that dynamic membrane biofilm formation not only improved the permeate quality but also played a significant role in MCCA production. *Clostridium* spp. were also found to be dominant in biofilms in a hollow-fiber membrane biofilm reactor used for MCCA production from  $\text{H}_2$  and  $\text{CO}_2$ , however, no comparison between the biofilm and suspended microbial communities was presented in that study.<sup>61</sup> Biofilms (either in dynamic membrane bioreactors or in other systems) support niche differentiation because of substrate gradients and may promote establishment of diverse MCCA populations. Biofilm growth may also provide protection from stress including MCCA toxicity, thus creating a favorable environment for chain elongating populations. Taken together, our microbial and MCCA data suggest that AnDMBRs have the potential to improve chain elongation by enriching for MCCA producing populations. Further investigation is needed to confirm the underlying mechanism responsible for higher MCCA production because of dynamic membrane formation.

## CONCLUSIONS AND ENGINEERING IMPLICATIONS

A laboratory-scale AnDMBR system was designed and operated to demonstrate MCCA production from a mixture of ethanol- and SCCA-rich waste streams and to produce a permeate with low suspended solids to enable direct integration of the AnDMBR with the MCCA extraction system. Directly integrating an AnDMBR with the extraction unit would decrease the environmental and physical footprint and cost compared to other chain elongation systems by eliminating the use of multiple external filters. Dynamic membrane formation led to high biomass retention, resulting in low permeate TSS concentration ( $0.12 \pm 0.06 \text{ g TSS L}^{-1}$ ) despite feeding high solids containing waste stream. The AnDMBR maintained stable performance for 224 days without fouling mitigation or cleaning, resulting in possibly lower

energy use and chemical consumption for fouling control compared to conventional membrane bioreactors. However, as the dynamic membrane became denser, the support meshes eventually clogged. Therefore, adopting some form of minimal cleaning such as backwashing, biogas recirculation, or intermittent operation to control the dynamic membrane thickness would be beneficial to ensure stable performance for an extended time. Our results show that high ( $>9 \text{ g L}^{-1}$ ) influent TSS concentration, which consequently affected MLSS concentration, negatively influenced dynamic membrane formation.

The AnDMBR dynamic membrane was enriched with highly active MCCA producing microbial populations such as *Clostridiales*. These observations were consistent with higher concentrations of MCCAs in the permeate compared to the bioreactor samples and suggest that chain elongation activity was promoted in the dynamic membrane biofilm. The results open up the possibility to further promote biofilm formation in bioreactor systems to enhance MCCA production. Biofilm morphology and structure, including EPS composition, need to be characterized to understand microbial interactions and their role in MCCA production. EPSs contribute to the formation of the dynamic membrane as shown by previous studies,<sup>60,62,63</sup> thereby affecting the performance of the system. Future characterization of the dynamic membrane layer, including an analysis of the EPS composition, would be helpful in developing control strategies to promote dynamic membrane formation and devise fouling mitigation strategies. Lastly, the laboratory-scale AnDMBR was operated at a low flux ( $0.4\text{--}0.7 \text{ L m}^{-2} \text{ h}^{-1}$ ), which would need to be increased for economical scale-up of the AnDMBR technology and improved efficiency of the downstream extraction unit.

## ASSOCIATED CONTENT

### Supporting Information

The Supporting Information is available free of charge at <https://pubs.acs.org/doi/10.1021/acsestengg.1c00273>.

Details about the bioreactor influent and inoculum, the pertraction system, and calculation on MCCA production, description of chemical and microbial analyses, characterization of inocula and influent, bioreactor operation parameters and performance data, and microbial analyses results (PDF)

## AUTHOR INFORMATION

### Corresponding Author

Lutgarde Raskin – Department of Civil and Environmental Engineering, University of Michigan, Ann Arbor, Michigan 48109, United States; [orcid.org/0000-0002-9625-4034](https://orcid.org/0000-0002-9625-4034); Email: [raskin@umich.edu](mailto:raskin@umich.edu)

### Authors

Shilva Shrestha – Department of Civil and Environmental Engineering, University of Michigan, Ann Arbor, Michigan 48109, United States; Present Address: Joint Bioenergy Institute, Emeryville, California 94608, United States; Biological Systems and Engineering Division, Lawrence Berkeley National Laboratory, Berkeley, California 94720, United States (S.S.); [orcid.org/0000-0001-5062-3634](https://orcid.org/0000-0001-5062-3634)  
Siqi Xue – Department of Civil and Environmental Engineering, University of Michigan, Ann Arbor, Michigan 48109, United States

**Dianna Kitt** – Department of Civil and Environmental Engineering, University of Michigan, Ann Arbor, Michigan 48109, United States

**Hang Song** – Department of Civil and Environmental Engineering, University of Michigan, Ann Arbor, Michigan 48109, United States; [orcid.org/0000-0002-9558-5827](https://orcid.org/0000-0002-9558-5827)

**Caro Truysers** – Department of Civil and Environmental Engineering, University of Michigan, Ann Arbor, Michigan 48109, United States; Department of Chemical Engineering, KU Leuven, Leuven 3001, Belgium

**Maxim Muermans** – Department of Civil and Environmental Engineering, University of Michigan, Ann Arbor, Michigan 48109, United States; Department of Chemical Engineering, KU Leuven, Leuven 3001, Belgium

**Ilse Smets** – Department of Chemical Engineering, KU Leuven, Leuven 3001, Belgium

Complete contact information is available at:

<https://pubs.acs.org/10.1021/acsestengg.1c00273>

## Notes

The authors declare no competing financial interest.

## ACKNOWLEDGMENTS

The authors would like to acknowledge Brittany Colcord for her help with preliminary bioreactor design, Steve Donajkowski, Ethan Kennedy, and Jan Pantolin for their assistance with building the AnDMBR system, and Doug Knox for providing waste beer. This study was financially supported by the U.S. National Science Foundation (Sustainability Research Networks 1444745). S.S. was supported by an Integrated Training in Microbial Systems Fellowship funded by the Boroughs Wellcome Fund, a Rackham Predoctoral Fellowship from the University of Michigan, and a Water Environment Federation Canham Graduate Studies Scholarship.

## REFERENCES

- (1) Angenent, L. T.; Richter, H.; Buckel, W.; Spirito, C. M.; Steinbusch, K. J. J.; Plugge, C. M.; Strik, D. P. B. T. B.; Grootsholten, T. I. M.; Buisman, C. J. N.; Hamelers, H. V. M. Chain Elongation with Reactor Microbiomes: Open-Culture Biotechnology to Produce Biochemicals. *Environ. Sci. Technol.* **2016**, *50*, 2796–2810.
- (2) Kucek, L.; Xu, J.; Nguyen, M.; Angenent, L. T. Waste Conversion into N-Caprylate and n-Caproate: Resource Recovery from Wine Lees Using Anaerobic Reactor Microbiomes and in-Line Extraction. *Front. Microbiol.* **2016**, *7*, 1892.
- (3) Ge, S.; Usack, J. G.; Spirito, C. M.; Angenent, L. T. Long-Term n-Caproic Acid Production from Yeast-Fermentation Beer in an Anaerobic Bioreactor with Continuous Product Extraction. *Environ. Sci. Technol.* **2015**, *49*, 8012–8021.
- (4) Xu, J.; Hao, J.; Guzman, J. J. L.; Spirito, C. M.; Harroff, L. A.; Angenent, L. T. Temperature-Phased Conversion of Acid Whey Waste Into Medium-Chain Carboxylic Acids via Lactic Acid : No External e-Donor. *Joule* **2018**, *2*, 280–295.
- (5) Andersen, S. J.; De Groof, V.; Khor, W. C.; Roume, H.; Props, R.; Coma, M.; Rabaey, K. A Clostridium Group IV Species Dominates and Suppresses a Mixed Culture Fermentation by Tolerance to Medium Chain Fatty Acids Products. *Front. Bioeng. Biotechnol.* **2017**, *8*, 8.
- (6) Angenent, L. T.; Usack, J. G.; Xu, J.; Hafenbradl, D.; Posmanik, R.; Tester, W. Integrating Electrochemical, Biological, Physical, and Thermochemical Process Units to Expand the Applicability of Anaerobic Digestion. *Bioresour. Technol.* **2018**, *247*, 1085–1094.
- (7) Urban, C.; Xu, J.; Sträuber, H.; dos Santos Dantas, T. R.; Mühlenberg, J.; Härtig, C.; Angenent, L. T.; Harnisch, F. Production of Drop-in Fuels from Biomass at High Selectivity by Combined Microbial and Electrochemical Conversion. *Energy Environ. Sci.* **2017**, *10*, 2231–2244.
- (8) Scarborough, M. J.; Lawson, C. E.; Hamilton, J. J.; Donohue, T. J.; Noguera, D. R. Metatranscriptomic and Thermodynamic Insights into Medium-Chain Fatty Acid Production Using an Anaerobic Microbiome. *mSystems* **2018**, *3* (), DOI: [10.1128/mSystems.00221-18](https://doi.org/10.1128/mSystems.00221-18).
- (9) Kucek, L.; Spirito, C. M.; Angenent, L. T. High N-Caprylate Productivities and Specificities from Dilute Ethanol and Acetate: Chain Elongation with Microbiomes to Upgrade Products from Syngas Fermentation. *Energy Environ. Sci.* **2016**, *9*, 3482–3494.
- (10) Lonkar, S.; Fu, Z.; Holtzapfel, M. Optimum Alcohol Concentration for Chain Elongation in Mixed-Culture Fermentation of Cellulosic Substrate. *Biotechnol. Bioeng.* **2016**, *113*, 2597–2604.
- (11) Barker, H. A.; Kamen, M. D.; Bornstein, B. T. The Synthesis of Butyric and Caproic Acids from Ethanol and Acetic Acid by Clostridium Kluyveri. *Proc. Natl. Acad. Sci. U. S. A.* **1945**, *31*, 373.
- (12) Wallace, R. J.; McKain, N.; McEwan, N. R.; Miyagawa, E.; Chaudhary, L. C.; King, T. P.; Walker, N. D.; Apajalahti, J. H. A.; Newbold, C. J. Eubacterium Pyruvivorans Sp. Nov., a Novel Non-Saccharolytic Anaerobe from the Rumen That Ferments Pyruvate and Amino Acids, Forms Caproate and Utilizes Acetate and Propionate. *J. Med. Microbiol.* **2003**, *53*, 965–970.
- (13) Genthner, B. R. S.; Davis, C. L.; Bryant, M. P. Features of Rumen and Sewage Sludge Strains of *Eubacterium Limosum*, a Methanol-Utilizing and H<sub>2</sub>-CO<sub>2</sub>-Utilizing Species. *Appl. Environ. Microbiol.* **1981**, *42*, 12–19.
- (14) Weimer, P. J.; Moen, G. N. Quantitative Analysis of Growth and Volatile Fatty Acid Production by the Anaerobic Ruminant Bacterium *Megasphaera Elsdenii* T81. *Appl. Microbiol. Cell Physiol.* **2013**, *97*, 4075–4081.
- (15) Shrestha, S. *Advancing Chain Elongation Technology for Medium Chain Carboxylic Acids Production from Waste Streams*; University of Michigan, 2020.
- (16) Kucek, L.; Nguyen, M.; Angenent, L. T. Conversion of L-Lactate into n-Caproate by a Continuously Fed Reactor Microbiome. *Water Res.* **2016**, *93*, 163–171.
- (17) De Sitter, K.; Garcia-Gonzalez, L.; Matassa, C.; Bertin, L.; De Wever, H. The Use of Membrane Based Reactive Extraction for the Recovery of Carboxylic Acids from Thin Stillage. *Sep. Purif. Technol.* **2018**, *206*, 177–185.
- (18) Ozgun, H.; Dereli, R. K.; Ersahin, M. E.; Kinaci, C.; Spanjers, H.; Van Lier, J. B. A Review of Anaerobic Membrane Bioreactors for Municipal Wastewater Treatment: Integration Options, Limitations and Expectations. *Sep. Purif. Technol.* **2013**, *118*, 89–104.
- (19) Smith, A. L.; Stadler, L. B.; Love, N. G.; Skerlos, S. J.; Raskin, L. Perspectives on Anaerobic Membrane Bioreactor Treatment of Domestic Wastewater: A Critical Review. *Bioresour. Technol.* **2012**, *122*, 149–159.
- (20) Ersahin, M. E.; Ozgun, H.; Dereli, R. K.; Ozturk, I.; Roest, K.; van Lier, J. B. A Review on Dynamic Membrane Filtration: Materials, Applications and Future Perspectives. *Bioresour. Technol.* **2012**, *122*, 196–206.
- (21) Hu, Y.; Wang, X. C.; Ngo, H. H.; Sun, Q.; Yang, Y. Anaerobic Dynamic Membrane Bioreactor (AnDMBR) for Wastewater Treatment: A Review. *Bioresour. Technol.* **2018**, *247*, 1107–1118.
- (22) Zhang, Y.; Zhao, Y.; Chu, H.; Dong, B.; Zhou, X. Characteristics of Dynamic Membrane Filtration: Structure, Operation Mechanisms, and Cost Analysis. *Chin. Sci. Bull.* **2014**, *59*, 247–260.
- (23) Cayetano, R. D. A.; Park, J. H.; Kang, S.; Kim, S. H. Food Waste Treatment in an Anaerobic Dynamic Membrane Bioreactor (AnDMBR): Performance Monitoring and Microbial Community Analysis. *Bioresour. Technol.* **2019**, *280*, 158–164.
- (24) Tang, J.; Wang, X. C.; Hu, Y.; Ngo, H. H.; Li, Y. Dynamic Membrane-Assisted Fermentation of Food Wastes for Enhancing Lactic Acid Production. *Bioresour. Technol.* **2017**, *234*, 40–47.



- (25) Paçal, M.; Semerci, N.; Çalli, B. Treatment of Synthetic Wastewater and Cheese Whey by the Anaerobic Dynamic Membrane Bioreactor. *Environ. Sci. Pollut. Res.* **2019**, *26*, 32942–32956.
- (26) Liu, H.; Wang, Y.; Yin, B.; Zhu, Y.; Fu, B.; Liu, H. Improving Volatile Fatty Acid Yield from Sludge Anaerobic Fermentation through Self-Forming Dynamic Membrane Separation. *Bioresour. Technol.* **2016**, *218*, 92–100.
- (27) Xie, Z.; Wang, Z.; Wang, Q.; Zhu, C.; Wu, Z. An Anaerobic Dynamic Membrane Bioreactor (AnDMBR) for Landfill Leachate Treatment: Performance and Microbial Community Identification. *Bioresour. Technol.* **2014**, *161*, 29–39.
- (28) Ersahin, M. E.; Ozgun, H.; Tao, Y.; van Lier, J. B. Applicability of Dynamic Membrane Technology in Anaerobic Membrane Bioreactors. *Water Res.* **2014**, *48*, 420–429.
- (29) Ersahin, M. E.; Gimenez, J. B.; Ozgun, H.; Tao, Y.; Spanjers, H.; van Lier, J. B. Gas-Lift Anaerobic Dynamic Membrane Bioreactors for High Strength Synthetic Wastewater Treatment: Effect of Biogas Sparging Velocity and HRT on Treatment Performance. *Chem. Eng. J.* **2016**, *305*, 46–53.
- (30) Carvajal-Arroyo, J. M.; Candry, P.; Andersen, S. J.; Props, R.; Seviour, T.; Ganigué, R.; Rabaey, K. Granular Fermentation Enables High Rate Caproic Acid Production from Solid-Free Thin Stillage. *Green Chem.* **2019**, *21*, 1330–1339.
- (31) Roghair, M.; Strik, D. P. B. T. B.; Steinbusch, K. J. J.; Weusthuis, R. A.; Bruins, M. E.; Buisman, C. J. N. Granular Sludge Formation and Characterization in a Chain Elongation Process. *Process Biochem.* **2016**, *51*, 1594–1598.
- (32) Wu, Q.; Feng, X.; Guo, W.; Bao, X.; Ren, N. Long-Term Medium Chain Carboxylic Acids Production from Liquor-Making Wastewater: Parameters Optimization and Toxicity Mitigation. *Chem. Eng. J.* **2020**, *388*, No. 124218.
- (33) Grootcholten, T. I. M.; Steinbusch, K. J. J.; Hamelers, H. V. M.; Buisman, C. J. N. Chain Elongation of Acetate and Ethanol in an Upflow Anaerobic Filter for High Rate MCFA Production. *Bioresour. Technol.* **2013**, *135*, 440–445.
- (34) Grootcholten, T. I. M.; Steinbusch, K. J. J.; Hamelers, H. V. M.; Buisman, C. J. N. High Rate Heptanoate Production from Propionate and Ethanol Using Chain Elongation. *Bioresour. Technol.* **2013**, *136*, 715–718.
- (35) Fonoll, X.; Meuwissen, T.; Aley, L.; Shrestha, S.; Raskin, L. The Rumen Membrane Bioreactor: Transforming Food Waste into Volatile Fatty Acids at the Small Scale. In *IWA 16th World Congress on Anaerobic Digestion*; The Netherlands, 2019.
- (36) Seluy, L. G.; Isla, M. A. A Process To Treat High-Strength Brewery Wastewater via Ethanol Recovery and Vinasse Fermentation. *Ind. Eng. Chem. Res.* **2014**, *53*, 17043–17050.
- (37) Eugene, W. R.; Rodger, B. B.; Andrew, D. E.; Lenore, S. C. *Standard Methods for the Examination of Water and Wastewater*; American Public Health Association (APHA): Washington, DC, USA, 2012.
- (38) Porebski, S.; Bailey, L. G.; Baum, B. R. Modification of a CTAB DNA Extraction Protocol for Plants Containing High Polysaccharide and Polyphenol Components. *Plant Mol. Biol. Report.* **1997**, *15*, 8–15.
- (39) Caporaso, J. G.; Lauber, C. L.; Walters, W. A.; Berg-Lyons, D.; Lozupone, C. A.; Turnbaugh, P. J.; Fierer, N.; Knight, R. Global Patterns of 16S RRNA Diversity at a Depth of Millions of Sequences per Sample. *Proc. Natl. Acad. Sci. U. S. A.* **2011**, *108*, 4516–4522.
- (40) Kozich, J. J.; Westcott, S. L.; Baxter, N. T.; Highlander, S. K.; Schloss, P. D. Development of a Dual-Index Sequencing Strategy and Curation Pipeline for Analyzing Amplicon Sequence Data on the Miseq Illumina Sequencing Platform. *Appl. Environ. Microbiol.* **2013**, *79*, 5112–5120.
- (41) Callahan, B. J.; McMurdie, P. J.; Rosen, M. J.; Han, A. W.; Johnson, A. J. A.; Holmes, S. P. DADA2: High-Resolution Sample Inference from Illumina Amplicon Data. *Nat. Methods* **2016**, *13*, 581–583.
- (42) Oksanen, J.; Blanchet, F. G.; Friendly, M.; Kindt, R.; Legendre, P.; McGlenn, D.; Minchin, P. R.; O'Hara, R. B.; Simpson, G. L.; Solyomos, P.; Stevens, M. H. H.; Szoeacs, E.; Wagner, H. *Package 'Vegan': Community Ecology Package. R Packag. version 2.5–6*, 2019. Available online: <https://github.com/vegandevs/vegan> (accessed on October 10, 2020)
- (43) McMurdie, P. J.; Holmes, S. Phyloseq: An R Package for Reproducible Interactive Analysis and Graphics of Microbiome Census Data. *PLoS One* **2013**, *8*, No. e61217.
- (44) Wickham, H.; Francois, R.; Henry, L.; Müller, K. *Dplyr: A Grammar of Data Manipulation. R Packag. version 1.0.5*, 2015, p. 156. Available online: <https://github.com/tidyverse/dplyr> (accessed on April 3, 2021)
- (45) Love, M. I.; Huber, W.; Anders, S. Moderated Estimation of Fold Change and Dispersion for RNA-Seq Data with DESeq2. *Genome Biol.* **2014**, *15*, 550.
- (46) Wickham, H.; Chang, W.; Henry, L.; Pedersen, T. L.; Takahashi, K.; Wilke, C.; Woo, K.; Yutani, H.; Dunnington, D. *Ggplot2: Create Elegant Data Visualisations Using the Grammar of Graphics Version 3.3.0*. 2016.
- (47) Ahmar Siddiqui, M.; Dai, J.; Guan, D.; Chen, G. Exploration of the Formation of Self-Forming Dynamic Membrane in an Upflow Anaerobic Sludge Blanket Reactor. *Sep. Purif. Technol.* **2019**, *212*, 757–766.
- (48) Guan, D.; Dai, J.; Watanabe, Y.; Chen, G. Changes in the Physical Properties of the Dynamic Layer and Its Correlation with Permeate Quality in a Self-Forming Dynamic Membrane Bioreactor. *Water Res.* **2018**, *140*, 67–76.
- (49) Van De Staey, G.; Smits, K.; Smets, I. An Experimental Study on the Impact of Biofloculation on Activated Sludge Separation Techniques. *Sep. Purif. Technol.* **2015**, *141*, 94–104.
- (50) Saleem, M.; Alibardi, L.; Cossu, R.; Lavagnolo, M. C.; Spagni, A. Analysis of Fouling Development under Dynamic Membrane Filtration Operation. *Chem. Eng. J.* **2017**, *312*, 136–143.
- (51) Cai, D.; Huang, J.; Liu, G.; Li, M.; Yu, Y.; Meng, F. Effect of Support Material Pore Size on the Filtration Behavior of Dynamic Membrane Bioreactor. *Bioresour. Technol.* **2018**, *255*, 359–363.
- (52) Roghair, M.; Liu, Y.; Strik, D. P. B. T. B.; Weusthuis, R. A.; Bruins, M. E.; Buisman, C. J. N. Development of an Effective Chain Elongation Process From Acidified Food Waste and Ethanol Into N-Caproate. *Front. Bioeng. Biotechnol.* **2018**, *6*, 1–11.
- (53) Altschul, S. F.; Gish, W.; Miller, W.; Myers, E. W.; Lipman, D. J. Basic Local Alignment Search Tool. *J. Mol. Biol.* **1990**, *215*, 403–410.
- (54) Liu, B.; Kleinstuber, S.; Centler, F.; Harms, H.; Sträuber, H. Competition Between Butyrate Fermenters and Chain-Elongating Bacteria Limits the Efficiency of Medium-Chain Carboxylate Production. *Front. Microbiol.* **2020**, *11*, 336.
- (55) Agler, M. T.; Spirito, C. M.; Usack, J. G.; Werner, J. J.; Angenent, L. T. Chain Elongation with Reactor Microbiomes: Upgrading Dilute Ethanol to Medium-Chain Carboxylates. *Energy Environ. Sci.* **2012**, *5*, 8189–8192.
- (56) Nzeteu, C. O.; Trego, A. C.; Abram, F.; O'Flaherty, V. Reproducible, High-Yielding, Biological Caproate Production from Food Waste Using a Single-Phase Anaerobic Reactor System. *Biotechnol. Biofuels* **2018**, *11*, 108.
- (57) Oz, N. A.; Ince, O.; Turker, G.; Ince, B. K. Effect of Seed Sludge Microbial Community and Activity on the Performance of Anaerobic Reactors during the Start-up Period. *World J. Microbiol. Biotechnol.* **2012**, *28*, 637–647.
- (58) Badel, S.; Bernardi, T.; Michaud, P. New Perspectives for Lactobacilli Exopolysaccharides. *Biotechnol. Adv.* **2011**, *29*, 54–66.
- (59) Czaczyk, K.; Myszka, K. Biosynthesis of Extracellular Polymeric Substances (EPS) and Its Role in Microbial Biofilm Formation. *Polish J. Environ. Stud.* **2007**, *16*, 799–806.
- (60) Ersahin, M. E.; Tao, Y.; Ozgun, H.; Spanjers, H.; van Lier, J. B. Characteristics and Role of Dynamic Membrane Layer in Anaerobic Membrane Bioreactors. *Biotechnol. Bioeng.* **2016**, *113*, 761–771.
- (61) Zhang, F.; Ding, J.; Zhang, Y.; Chen, M.; Ding, Z. W.; van Loosdrecht, M. C. M.; Zeng, R. J. Fatty Acids Production from Hydrogen and Carbon Dioxide by Mixed Culture in the Membrane Biofilm Reactor. *Water Res.* **2013**, *47*, 6122–6129.



(62) Lin, H. J.; Xie, K.; Mahendran, B.; Bagley, D. M.; Leung, K. T.; Liss, S. N.; Liao, B. Q. Factors Affecting Sludge Cake Formation in a Submerged Anaerobic Membrane Bioreactor. *J. Membr. Sci.* **2010**, *361*, 126–134.

(63) Zhang, X.; Wang, Z.; Wu, Z.; Lu, F.; Tong, J.; Zang, L. Formation of Dynamic Membrane in an Anaerobic Membrane Bioreactor for Municipal Wastewater Treatment. *Chem. Eng. J.* **2010**, *165*, 175–183.

**HAZARD AWARENESS  
REDUCES LAB INCIDENTS**

**ACS Essentials of  
Lab Safety for  
General Chemistry**

A new course from the  
American Chemical Society

ACS Institute  
Learn. Develop. Excel.

EXPLORE  
ORGANIZATIONAL  
SALES  
[solutions.acs.org/essentialsoflabsafety](https://solutions.acs.org/essentialsoflabsafety)

REGISTER FOR  
INDIVIDUAL ACCESS  
[institute.acs.org/courses/essentials-lab-safety.html](https://institute.acs.org/courses/essentials-lab-safety.html)